scientific reports

Check for updates

OPEN

The m6A reader IGF2BP3 promotes HCC progression by enhancing MCM10 stability

Lianwu Zhao[1,2], Hongyan Huang[1,2], Linfei Luo[1,2], Zixiang Huang[1,2], Zhengqiang Wu[1], Fenfen Wang[1] & Zhili Wen[1]✉

Abnormal N6-methyladenosine (m6A) modifications were associated with the occurrence, development, and metastasis of cancer. However, the functions and mechanisms of m6A regulators in cancer remained largely elusive and should be explored. Here, we identified that insulin like growth Factor 2 mRNA binding protein 3 (IGF2BP3) was specifically overexpressed and associated with poor prognosis in liver hepatocellular carcinoma (HCC). Importantly, IGF2BP3 promoted HCC cells progression in an m6A-dependent manner, IGF2BP3 silencing significantly inhibited proliferation and migratory ability of tumor cells in vitro and in in vivo. Mechanistically, IGF2BP3 interacted with minichromosomal maintenance complex component (MCM10) mRNAs to prolong stability of m6A-modified RNA. Therefore, our findings indicated that m6A reader IGF2BP3 contributed to tumorigenesis and poor prognosis, providing a potential prognostic biomarker and therapeutic target for HCC.

Keywords HCC, IGF2BP3, MCM10, m6A modification

liver hepatocellular carcinoma (HCC) is one of the most prevalent lethal tumors, with Chinese HCC patients accounting for 50% of global cases[1,2]. Although treatments have improved significantly recently, the efficacy is still far from ideal[3]. Therefore, it is imperative to further illustrate the molecular pathogenesis of HCC to develop novel therapeutic strategies.

Emerging evidence has demonstrated that dysregulated m6A-associated proteins and m6A modifications play a crucial role in the initiation and progression of cancer[4]. N6-methyladenosine (m6A) modifications are dynamic and reversible posttranscriptional RNA modifications that are mediated by m6A regulators, such as methyltransferases ("writers": METTL3, METTL14, and WTAP), demethylases ("erasers": ALKBH5 and FTO), and m6A-binding proteins ("readers": YTHDs and IGF2BPs)[5,6]. IGF2BP3, a protein of recognizing the m6A modified sites on RNA transcripts, can determine the cellular fate of target mRNAs via regulating splicing, nuclear exportation, degradation, stabilization, and translation of RNA molecules[7]. To date, the role of various m6A reader proteins in the progression of HCC remains largely unexplored. Therefore, it is necessary to elucidate the biological importance of m6A regulators in promoting tumors.

MCM10 was an evolutionary conserved protein required for DNA replication in eukaryotes[8]. Recently, MCM10 was demonstrated to tightly bind CMG, forming a CMG-MCM10 complex (CMGM), which stimulated both CMG helicase activity and the rate of the replisome[9,10]. In addition, MCM10 played important role in replisome stability, fork progression, and DNA repair[11–15].

Here, we demonstrated that a critical m6A reader, insulin like growth Factor 2 mRNA binding protein 3 (IGF2BP3) directly recognized m6A modified mRNAs of MCM10 gene and stabilized MCM5 mRNAs to contribute to tumorigenesis in HCC. In summary, our results revealed that m6A modulation on cancer cell plasticity and provided potential therapeutic targets for HCC.

Materials and methods

Data collection

mRNA-seq datasets and clinical information of HCC were obtained from the Cancer Genome Atlas (TCGA) database (https://cancergenome.nih.gov/).

[1]Department of Gastroenterology, The 2nd Affiliated Hospital, Jiangxi Medical College, Nanchang University, Jiangxi 330000, People's Republic of China. [2]Lianwu Zhao, Hongyan Huang, Linfei Luo, and Zixiang Huang contributed equally to this work. ✉email: wenzhili@126.com

Construction of a protein-protein interaction (PPI) network
The mRNAs were included in a PPI network using the STRING database (https://string-db.org/) with a confidence score of > 0.8. Cytoscape (version 3.8.1) was used to visualise the PPI network[16].

Survival analysis
The difference in overall survival (OS) between the two groups was evaluated by Kaplan-Meier survival analysis using the log-rank test.

Evaluation of predictive ability
Receiver operating characteristic (ROC) curves based on the survivalROC package were applied to assess the predictive performance of IGF2BP3 within 0.5, 1, and 1.5 years. Univariate Cox regression analysis and multivariate Cox regression analysis was performed to evaluate the resolution of IGF2BP3.

Gene set variation analysis (GSVA)
GSVA analysis was used to investigate the variation in biological processes between different cuproptosis regulation patterns with the R package 'GSVA' and KEGG software (www.kegg.jp/kegg/kegg1.html).

DEGs analysis
The "limma" package of R software was used to identify the DEGs between high-IGF2BP3 and low-IGF2BP3 expression groups. The top 100 up-regulated and down-regulated genes were screened.

Cell culture and cell culture
Human hepatic carcinoma cells lines (HCCL-M3 and Huh-7 cells.) were purchased from the Chinese Academy of Sciences Cell Bank and cultured in Dulbecco's modified Eagle's medium (DMEM) (Invitrogen) containing 10% FBS (HyClone) and 1% penicillin–streptomycin (P/S).

Colony formation assay
For the colony formation assay, transfected cells ($5 \times 10\text{^}3$ cells/well) were cultured in 6-well plate. The resulting colonies were washed twice with PBS and fixed with 4% formaldehyde for 10 min and stained for 30 min with 0.1% crystal violet. The colonies were photographed and counted.

CCK-8 assay
To evaluate cell viability, we employed Cell Counting Kit-8 (APEBIO, USA) according to the manufacturer's instructions. Briefly, 1×10^4 pretreated cells were seeded into 96-well plates, and the volume of medium added to each well was 100 µL. Next day, the cells were incubated for 2 h at 37 °C, after adding10 µL CCK8 solution in each well. Finally, absorbance (450 nm) was measured by SpectraMax i3x reader.

Transwell migratory experiment
To evaluate cell migratory ability, HCCL-M3 and Huh-7 cells (3×10^4) were seeded into the upper chamber and incubated overnight. Subsequently, 500 µL complete medium supplemented with 10% FBS was added into the lower chamber of the Transwell insert to promote cell migration. After 24 h, cells migrating through the membrane of Transwell inserts were stained with crystal violet and photographed by microscopy.

Wound healing assay
Cells were seeded in 6-well plate and incubated overnight. Next day, the inserts were removed, and serum-free medium was added. After 36 h. ImageJ was used to calculate the migratory rate.

Western blot
RIPA buffer (Beyotime, Shanghai) was used to extract total protein from cells, then the protein concentration was detected by the BCA kit (Beyotime, China). Protein samples were separated by SDS-PAGE and transferred to polyvinylidene fluoride (PVDF) membranes. Primary antibodies against specific genes were diluted and incubated with PVDF membranes overnight at 4 °C. The next day, the membranes were incubation with secondary antibody at room temperature for 2 h. Original western blot images are listed in Supplementary Figure S1.

Chemical reagents, antibodies, and transfection
HUR (Ribobio, Guangzhou, China); actinomycin D (APExBio, Houston, TX, USA); anti-IGF2BP3 (Abcam, Cambridge, UK); IGF2BP3 overexpression plasmids and short hairpin RNA (shRNA) were purchased from GeneChem (Shanghai, China). The specific human shRNA sequences (shIGF2BP3: ATATCCCGCCTCATTTA CAG). All transfections were performed according to the manufacturers' instructions.

Quantitative RT–PCR
Total RNA was extracted from cells using TRIzol reagent (Invitrogen, USA) according to the manufacturer's instructions. 1 µg of RNA was applied for reverse transcription (Cat. #R323-01, Vazyme). Real-time PCR analysis was performed using SYBR Premix Ex TaqTM (Tli RNaseH Plus) (TaKaRa, Dalian, China). The amplification primers (IGF2BP3 forward: GGGAGGTGCTGGATAGTTTAC; IGF2BP3 reverse: CTAGCTTGGTCCTTACT GGAATAG).

RNA Immunoprecipitation (RIP) assay

The Geneseed RIP Kit (Guangzhou, China) was performed for the RIP assay according to the instructions. Briefly, magnetic beads were mixed with anti-m6A/IGF2BP3/IgG antibodies, and then added cell lysates. Next, the bound complexes were thoroughly washed, eluted, purified, and analyzed by RT–qPCR. Enrichment of precipitated RNAs was normalized relative to input controls.

mRNA stability assay

To explore the stability of MCM10 mRNA and protein under the downregulation or upregulation of IGF2BP3, cells were treated with actinomycin D for 0, 3, 6 h prior to RNA extraction. The procedures of total RNA isolation and RT-qPCR were performed as described above. The transcript level of MCM10 mRNA was estimated as the half-life of the mRNA and normalized to GAPDH as the standard.

Tumor xenograft model

Animal experiments are approved by the Ethics committee and carried out in strict accordance with the requirements. Male BALB/c nude mice (4–6 weeks, 18–22 g) purchased from the animal center of Biotechnology Co., Ltd (Beijing, China) were maintained under specific pathogen-free conditions. Treated Huh-7 cell suspensions (1×10^6 cells) were mixed 1:1 and injected subcutaneously into the right axillae of nude mice. Quantification of immunohistochemical staining was performed using Image-Pro Plus 6.0 software. Tumor volume was calculated as follows: (longest diameter) × (shortest diameter)2 × (π/6). All animal experimental procedures used in this study were approved by the Animal Ethics Committee of the Second Affiliated Hospital, Jiangxi Medical College, Nanchang University. All methods were performed in accordance with the ARRIVE guidelines and related guidelines and regulations.

Statistical analysis

Statistical analyses were performed using R, version 4.2.3. Survival analysis was performed by the Kaplan–Meier method with a log rank test. Correlations were analyzed by using Pearson's correlation. Univariate and multivariable survival analysis were performed using Cox regression analysis. A two-tailed Student's t-test was used to compare between groups for statistical significance. All experiments were performed for at least 3 times independently under similar conditions, unless otherwise specified in the figure captions. In all cases, p value < 0.05 was considered statistically significant.

Results

High-throughput library screening identifies IGF2BP3 as a core m6A regulator in HCC

A total of 26 m6A regulators including 10 writers, 3 erasers and 13 readers were finally identified based on TCGA data in this study. The process of m6A methylation was dynamically and reversibly regulated by these m6A regulators (Fig. 1a and Table-S1). The investigation of CNV alteration frequency revealed a prevalent CNV alteration in 26 regulators. VIRMA, HNRNPC, and METTL3 showed copy number deletions, whereas ZC3H13 and YTHDF2 had CNV amplification frequencies (Fig. 1b). Compared to normal tissues, m6A regulators with amplificated CNV demonstrated remarkedly higher expression in HCC tissues, and vice versa (Fig. 1b and c). The comprehensive landscape of m6A regulator interactions, regulator connection and their prognostic significance for HCC patients was depicted with the m6A regulator network. We found m6a regulators that not only exhibited significant correlations in expression within the same functional category but also between writers, erasers, and readers. (Fig. 1d and Table S). By joint difference, survival, risk, and prognosis analysis, we screened out IGF2BP3 as the only significant regulated gene (Fig. 1e). A survival analysis showed that patients with high IGF2BP3 expression exhibited worse overall survival (Fig. 1f). Taken together, these data further reveal an oncogenic role for IGF2BP3 in tumour progression.

IGF2BP3 was an independent prognostic factor in HCC

Based on the TCGA dataset, high IGF2BP3 expression was related with higher risk score and poorer OS status in HCC patients (Fig. 2a). In addition, receiver operating characteristics (ROC) curve analysis of the promising predictive value for IGF2BP3 expression showed that the areas under the curves (AUCs) for 0.5-, 1-, and 1.5-year OS were 0.682, 0.669, and 0.619, respectively (Fig. 2a). The multi-index ROC analysis revealed that the AUC of IGF2BP3 was significantly better than those of other clinicopathological indicators (Fig. 2a) (such as age, gender, and stage). In univariate Cox analysis, stage ($p < 0.01$) and risk score ($p < 0.001$) were significantly correlated with OS (Fig. 2c). In multivariate Cox analysis, only IGF2BP3 ($p < 0.001$) was an independent prognostic factor (Fig. 2d). Together, these data illustrate IGF2BP3 is an independent prognostic factor in HCC.

IGF2BP3 promoted tumor progression in HCC

To explore the biological function of IGF2BP3 in HCC, we transfected IGF2BP3 knockdown or overexpression in HCCL-M3 and Huh-7 cells. Transfection efficiency was evaluated by western blot and qPCR (Fig. 3a-b and Figure S1). Colony formation assays and CCK-8 showed that IGF2BP3 played a vital role in cell proliferation and colony formation ability (Fig. 3c-d). In addition, IGF2BP3 also impacted cell migratory ability in HCCL-M3 and Huh-7 cells (Fig. 3e-g). The Huh-7 cell suspension mixtures were used to establish an in vivo xenograft model. During the observation of flank xenografts in BALB/c nude mice for 28 days, IGF2BP3 knockdown significantly delayed tumor progression, as the volume of IGF2BP3-deficient tumors was significantly decreased compared with that of control tumors (Fig. 3h-i). The nude mice were sacrificed, and the xenografts were harvested and weighed, the results showed tumor weights was significantly reduced (Fig. 3j). Therefore, these data illuminated that IGF2BP3 promoted tumor progression in HCC.

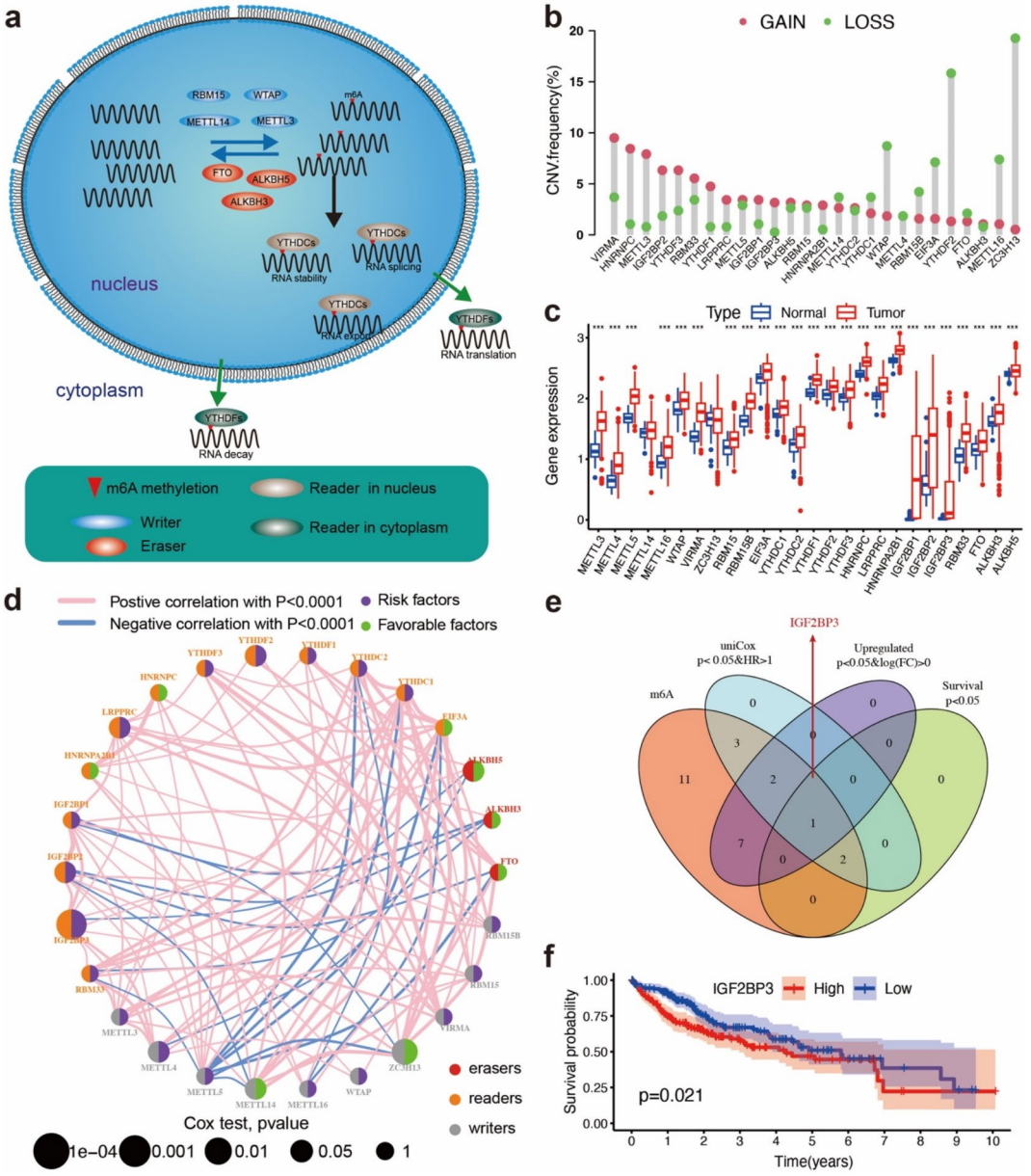

Fig. 1. High-throughput library screening identifies the key m6A regulator in HCC. (**a**) Essential regulators in m6A RNA methylation events, and their biological functions. (**b**) The CNV variation frequency of m6A regulators in TCGA cohort. The height of the column represented the alteration frequency. The deletion frequency, blue dot; The amplification frequency, red dot. (**c**) Differential expression of m6a regulators between normal and HCC tissues. HCC, red; Normal, blue. Significant results are indicated as $^{***}p < 0.001$. (**d**) The interaction of expression on 28 m6A regulators in HCC. Different biological functions of m6A regulators were depicted by circles in different colors. The lines linking regulators showed their interactions, pink represented positive correlation, and blue represented negative correlation. The circle size represented the effect of each regulator on the prognosis by P-value. Purple dots in the circle showed risk factors of prognosis; Green dots in the circle showed favorable factors of prognosis. (**e**) The Venn plot showed IGF2BP3was identified based on the intersection analysis. Cox, $p < 0.05$; HR > 1; differential analysis, Log (FC) > 0, $p < 0.05$. (**f**) Kaplan–Meier survival analysis showed that IGF2BP3 exhibited prognosis in HCC patients based on TCGA data.

Functional annotations of IGF2BP3 in HCC

The correlations between IGF2BP3 expression and clinical properties were examined in the TCGA dataset. High IGF2BP3 expression level was related with older age, gender, and tumor stage (Fig. 4a). Single-sample GSEA (ssGSEA) algorithm was used to evaluate the associations between IGF2BP3 expression and immune cell infiltration, the results showed that the immune activity of patients with high IGF2BP3 seemed to be slightly increased compared with that of patients with low IGF2BP3 (Fig. 4b), but there is no statistical significance, which

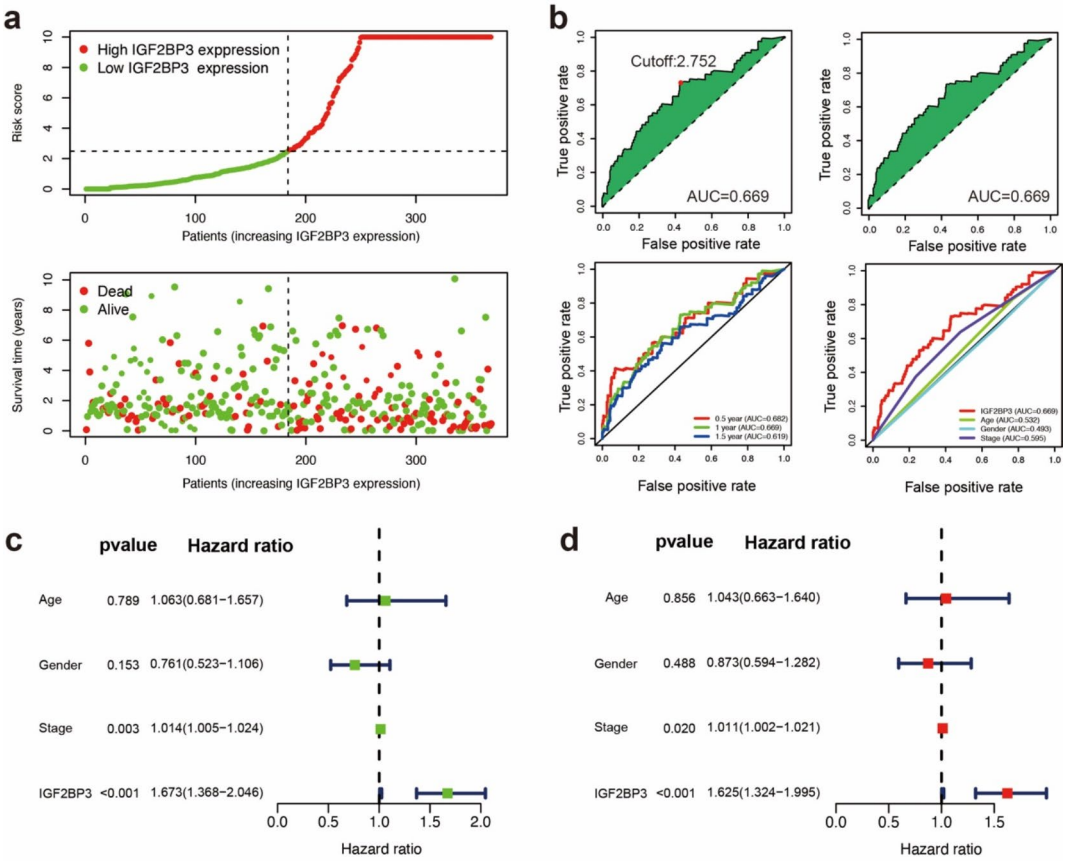

Fig. 2. IGF2BP3 is an independent prognostic factor in HCC. (**a**) Distribution of risk score, OS, and OS status in the high and low IGF2BP3 subgroups. (**b**) The AUC value and cutoff point obtained in the TCGA set, ROC curve analysis within 0.5, 1, and 1.5 years, and multivariate ROC curve analysis showing that the superior prognostic performance of the IGF2BP3 expression compared to other clinical indicators. (**c**) Univariate analysis of the IGF2BP3 expression and other clinical information in TCGA HCC cohort. (**d**) Multivariate analysis of the IGF2BP3 expression and other clinical information in TCGA HCC cohort.

suggested that IGF2BP3 did not promote tumor progression by regulating the immune system. Additionally, Gene set variation analysis (GSVA) was performed to explore the underlying molecular mechanisms differing in the high-IGF2BP3 and low-IGF2BP3 subgroups of HCC patients. The results showed that high-IGF2BP3 patients were mainly related with mitotic spindle, G2M checkpoint, E2F targets, and cell cycle signaling pathway in the TCGA dataset (Fig. 4c-d).

Protein–protein interaction network and univariate Cox regression analyses

To further investigate the potential biological behavior of IGF2BP3 modification pattern, we determined the top 200 DEGs between high-IGF2BP3 and low-IGF2BP3 expression groups using limma package. The PPI network of the interactions among 200 DEGs was performed using STRING database (confidence value > 0.8) (Fig. 5a), which were visualized in Cytoscape v3.8.2 (Fig. 5b). The top 30 genes were represented based on the number of nodes using bar plots, which may serve as hub nodes in the network (Fig. 5c and Table **S2**). In addition, univariate Cox regression analyses showed that 23 genes were of prognostic significance among the 200 DEGs (Fig. 5d and Table S3).

IGF2BP3 regulated MCM10 expression in an m6A-dependent manner

Based on previous studies, 51 genes were identified as transcripts recognized and regulated by IGF2BP3 through m6A modification[17]. MCM10 was identified based on the intersection of the prognostic significance, the top 30 hub genes in the PPI network, and 51 genes of IGF2BP3 through m6A modification (Fig. 6a). Subsequently, the expression and potential role of MCM10 were further explored using the TCGA dataset. The expression of MCM10 was significantly increased in HCC comparing normal tissue (Fig. 6b-c). K-M analysis showed that HCC patients with MCM10 overexpression had poor survival (Fig. 6d). The distinct m6A sites in MCM10 at single-base resolution were predicted using m6A site prediction tool SRAMP[18] (Fig. 6e).Then, MeRIP-RT–qPCR was performed to investigate whether gene expression affected m6A modification, the results indicated MCM10 mRNA enrichment in the m6A-specific antibody precipitate (Fig. 6f). RIP and RT–qPCR was used to evaluate RNA enrichment, the results showed that the mRNA of MCM10 was enriched by the anti-IGF2BP3 antibody compared with IgG in the HCCL-M3 and Huh-7 cell lines, which confirmed the direct interaction

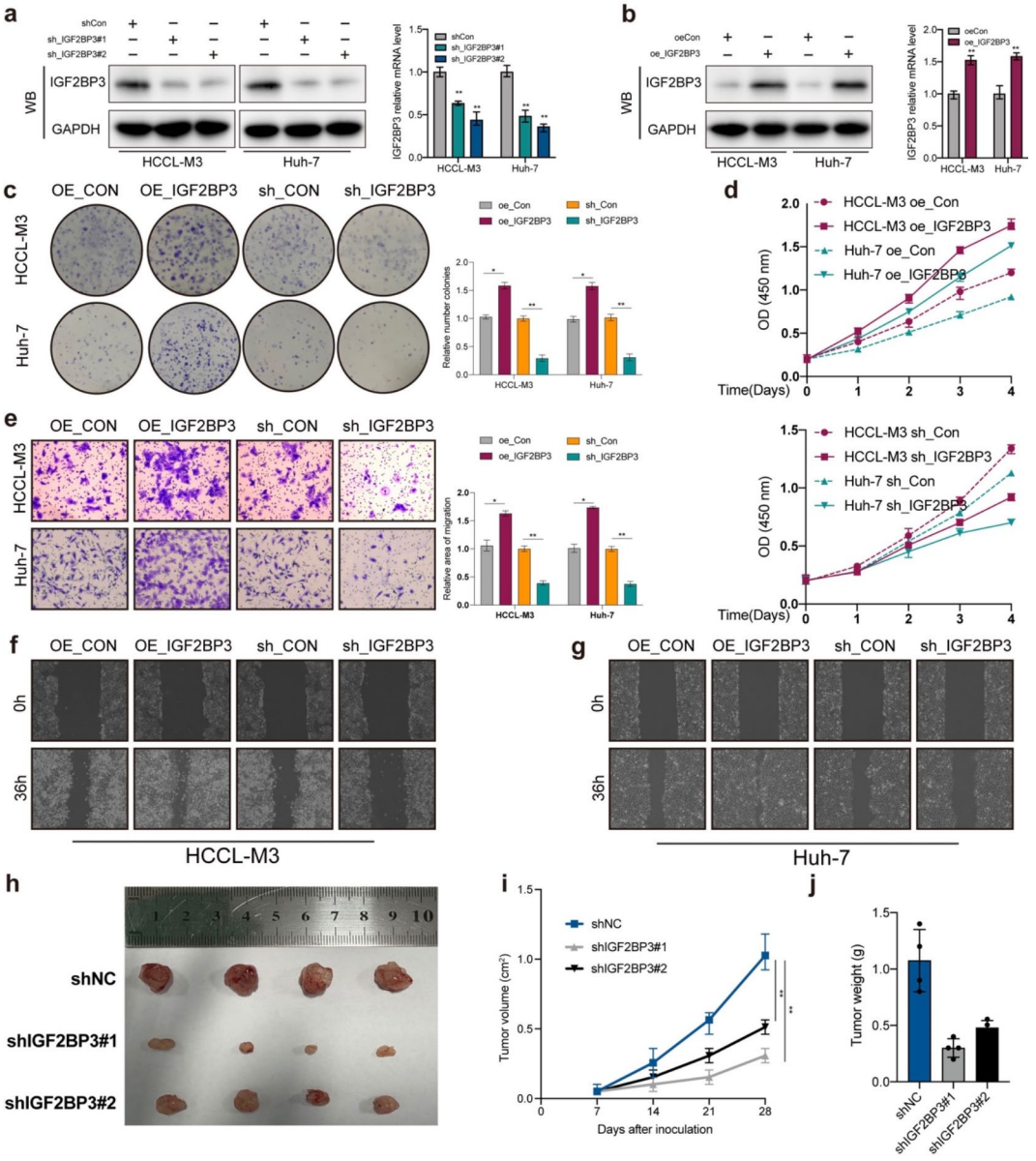

Fig. 3. IGF2BP3 promotes tumor progression in HCC. (**a**) Transfection knockdown efficiencies was validated in HCCL-M3 and Huh-7 cells by western blot and qPCR, respectively. (**b**) Transfection overexpression efficiencies was validated in HCCL-M3 and Huh-7 cells by western blot and qPCR, respectively. (**c**-**d**) CCK-8 and colony formation assay was used to analyze the proliferation viability of IGF2BP3 in HCC cell. (**e**-**g**) Transwell migration assay and wound healing assay was used to analyze the migration viability of IGF2BP3 in HCC cell. (**h**) The image of mice bearing subcutaneous tumors derived from Huh-7 cells treated with different treatment (shNC, shIGF2BP3#1, or shIGF2BP3#2) at the indicated times. (**i**) The xenograft growth curves for the shIGF2BP3#1, shIGF2BP3#2, and shNC groups were plotted by measuring the tumor size (width2 × length × π/6) with a Vernier caliper every 7 days. (**j**) Nude mice were sacrificed, and xenografts were harvested and weighed. All the data are presented as the mean ± standard deviation ($n = 3$). $^{*}P < 0.05$, $^{**}P < 0.01$, compared with the control group.

between IGF2BP3 and MCM10 (Fig. 6g). IGF2BP3 overexpression markedly prolonged (Fig. 6h), while IGF2BP3 knockdown obviously shortened the half-life of MCM10 mRNA in HCC cells (Fig. 6i). Moreover, silencing mRNA stabilizer HuR dramatically diminished IGF2BP3-induced MCM10 upregulation (Fig. 6j), which demonstrated IGF2BP3 regulated MCM10 expression by modulating its mRNA stability. As expected, IGF2BP3 knockdown markedly inhibited the expression level of MCM10 protein (Fig. 6g). By contrast, IGF2BP3 overexpression remarkably enhanced the expression level of MCM10 protein (Fig. 6h). Taken together, these dates revealed that IGF2BP3 mediated the degradation of MCM10 mRNA to maintain its protein level by m6A modification.

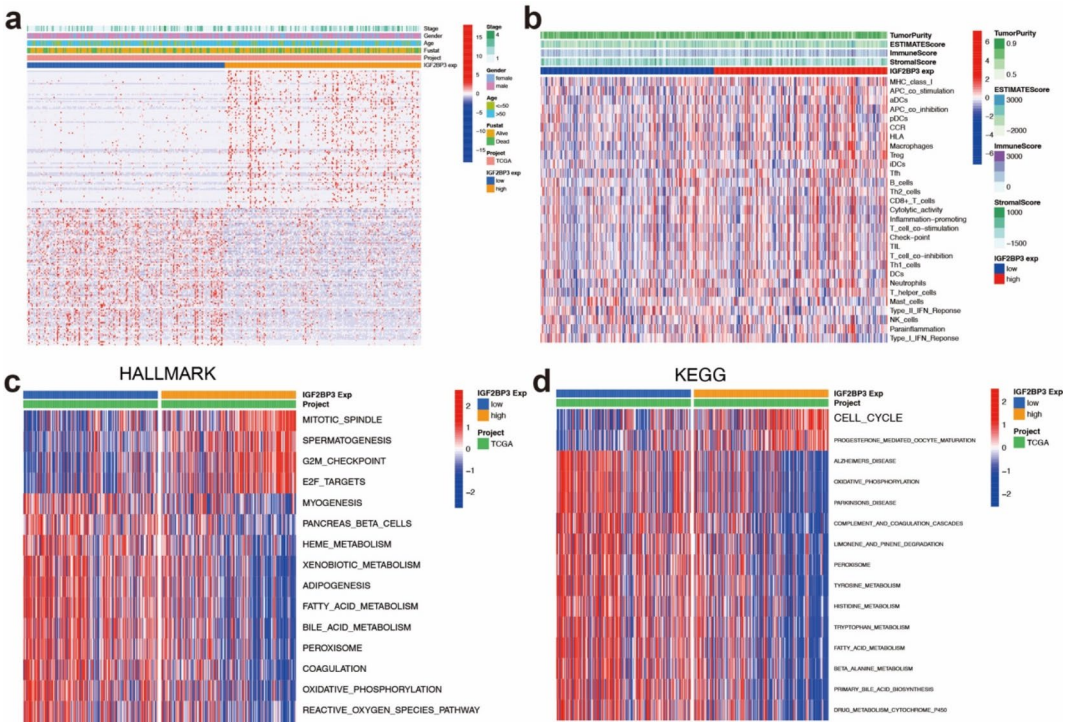

Fig. 4. Functional annotations of IGF2BP3 in HCC. (**a**) Associations between IGF2BP3 expression and clinical features of HCC based on TCGA data. (**b**) Correlations between IGF2BP3 expression and immune-interrelated signatures, as determined by ESTIMATE, immune, stromal, and tumor purity scores based on TCGA data. (**c**) GSVA analyses (HALLMARK) of IGF2BP3 in HCC patients based on TCGA data. (**d**) GSVA analyses (KEGG, www.kegg.jp/kegg/kegg1.html) of IGF2BP3 in HCC patients based on TCGA data.

IGF2BP3 promoted HCC progression through MCM10 expression

Since IGF2BP3 could regulate MCM10 expression, rescue experiments were carried out to verify the interaction between IGF2BP3 and MCM10 in HCC progression. As expected, MCM10 could partially counteract the antitumor effects on cell viability (Fig. 7a), colony formation (Fig. 7b) and migration (Fig. 7c-d) mediated by shIGF2BP3. In addition, overexpression of MCM10 also promoted cell proliferation, colony formation and migration in HCCL-M3 and Huh-7 cells, confirming the oncogenic effects of MCM10 (Fig. 7a-d). Importantly, in BALB/c mice's model, IGF2BP3 overexpression-induced tumor progression could be partially abrogated by MCM10 knockdown (Fig. 7e-g). Collectively, IGF2BP3 promotes HCC progression through MCM10 expression.

Discussion

N6-methyladenosine (m6A) modification, as crucial regulators of hepatocellular carcinoma development, highlight the importance of understanding the crosstalk between these biological processes[19]. Accumulating evidence has indicated that IGF2BP3 is highly expressed and promotes tumor progression in HCC[19,20], however, the role of IGF2BP3 is not well understood.

In this study, among 26 m6A regulators (writers:10, erasers:3 and readers:13), we firstly identified the key m6A regulator IGF2BP3 in HCC using TCGA dataset through CNV alteration frequency, differential analysis, correlation analysis, and survival analysis. Then, we demonstrated that IGF2BP3 was an independent prognostic factor in hepatocellular carcinoma based on ROC curve, univariate analysis, and multivariate analysis. IGF2BP3 has been confirmed to be overexpressed in a variety of tumors and affects patient prognosis, such as breast cancer[21], Gastric cancer[22], and glioma[23]. We confirmed bioinformatically that the IGF2BP3 expression was significantly higher in hepatocellular carcinoma tumor samples than in normal samples, and patients with high IGF2BP3 expression had a worse prognosis. In vitro experiments, we demonstrated that IGF2BP3 promoted tumor progression in HCC by CCK-8, colony formation assay, transwell migration assay, and wound healing assay.

Next, we further explored the function of IGF2BP3 in hepatocellular carcinoma, the results showed older age, gender, and tumor stage were positive with IGF2BP3 expression level. Surprisingly, high-IGF2BP3 expression were no obvious immune activity compared to low-IGF2BP3 patients. In addition, GSVA showed high-IGF2BP3 patients were mainly related with mitotic spindle, G2M checkpoint, E2F targets, and cell cycle signaling pathway.

To further investigate the modification pattern of IGF2BP3, the total of 200 DEGs were screened between high-IGF2BP3 and low-IGF2BP3 expression groups, and then subjected to the PPI network analysis and univariate Cox regression analyses. Finally, the top 30 key genes and 23 prognostic genes were identified. IGF2BP3, as regulator ("reader") of m6A modification, has been reported to play an important role in tumor

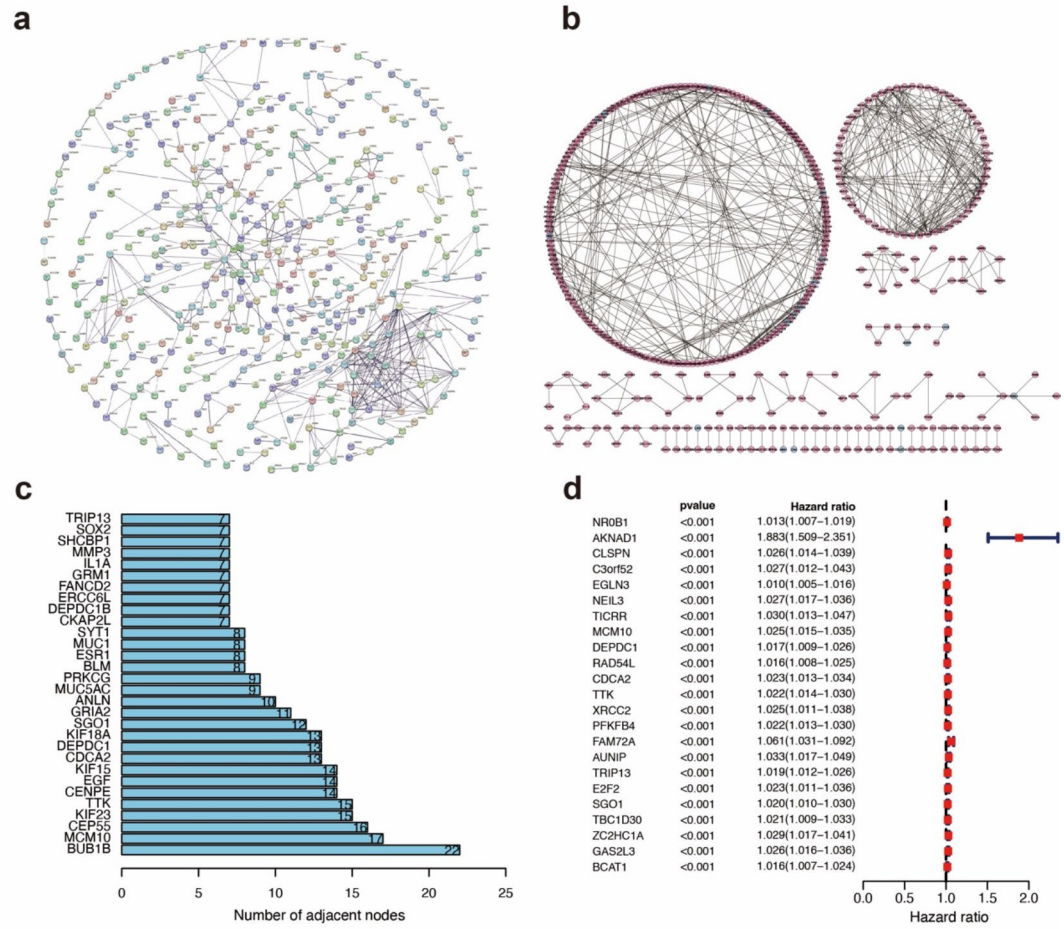

Fig. 5. Protein–protein interaction network and univariate cox regression analyses. (**a**) The PPI network based on the STRING confidence score > 0.9. (**b**) The visualization of the PPI network. (**c**) The top 30 genes ordered by the number of nodes. (**d**) Univariate Cox analyses of 200 DEGs.

progression[17,24,25]. Such as, in non-small cell lung cancer (NSCLC), IGF2BP3 interacted with STRIP2 to regulate TMBIM6 mRNA stability in an m6A-dependent manner[25]. IGF2BP3 contributed to the tumorigenesis and poor prognosis of acute myeloid leukemia (AML) by changing the stability of RCC2 mRNA in an m6A-dependent manner[24]. So, we explored whether IGF2BP3 regulated progression of hepatocellular carcinoma via m6A-dependent manner. After combined analysis of node genes, prognostic genes, and IGF2BP3 with m6A -modified gene, MCM10 was identified as being modified by IGF2BP3 with m6a in HCC. Minichromosome maintenance protein 10 (MCM10), a member of the MCM family, is essential for DNA replication[26]. We confirmed bioinformatically that MCM10 was significantly upregulated in HCC comparing normal tissue, and MCM10 overexpression showed poor survival. MeRIP-RT–qPCR demonstrated that IGF2BP3 modulated MCM10 mRNA stability via m6A modification. Importantly, in vitro experiments, rescue experiments were carried out to verify IGF2BP3 promotes HCC progression through MCM10 expression. Above data suggested IGF2BP3-MCM10 axis has an important role in HCC progression and provides a novel potential prognostic biomarker for hepatocellular carcinoma.

Conclusion

In summary, we demonstrated that the m6A reader IGF2BP3 contributes to the tumorigenesis and poor prognosis of HCC by maintaining MCM10 mRNA stability, providing a distinct mechanistic insight in m6A-dependent, which should be helpful for developing MCM10 signaling-targeted inhibitors.

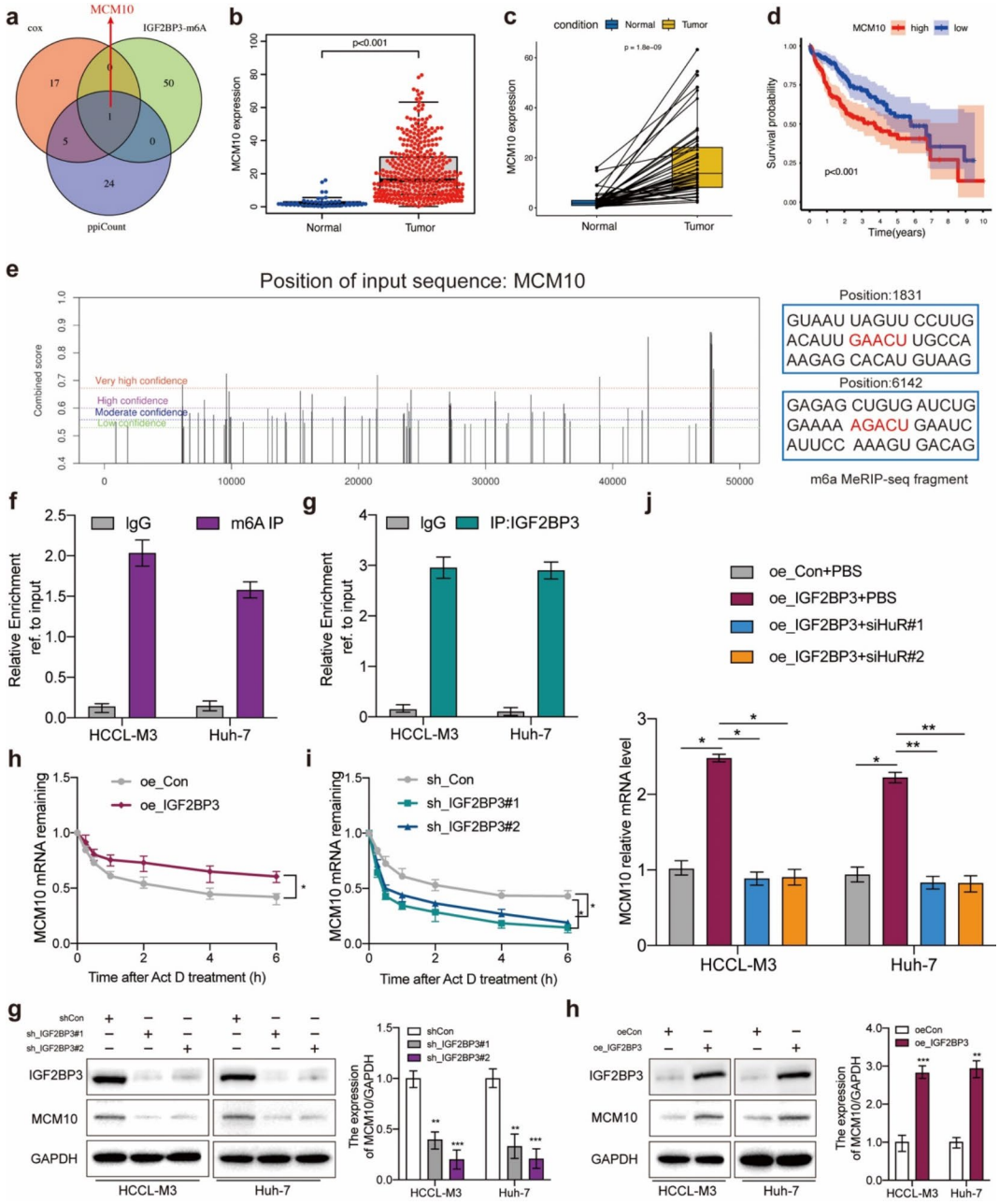

Fig. 6. MCM10 had Potential to be an Indicator of IGF2BP3 modulation. (**a**) The Venn plot showed MCM10 was identified based on the intersection analysis in TCGA data. (**b**-**c**). The expression of MCM10 between normal and tumor tissues in TCGA data. (**d**) The survival analysis of HCC patients with low and high MCM10 expression in TCGA data. (**e**) The potential m6A sites in MCM10 were predicted by SRAMP. The different colored lines indicate different confidence levels. (**f**) The mRNA of MCM10 was enriched by the m6A-specific antibody compared to IgG in HCCL-M3 and Huh-7 cells. (**g**) The mRNA of MCM10 was enriched by the anti-IGF2BP3 antibody compared to IgG in HCCL-M3 and Huh-7 cells. (**h**-**i**). qRT-PCR assay showing MCM10 mRNA stability in HCCL-M3 cells. (**j**) The effect of silencing HuR on MCM10 expression in HCCL-M3 and Huh-7 cells. (**g**-**h**). The expression of MCM10 protein under the presence of IGF2BP3 knockdown (**g**) or overexpression (**h**). All the data are presented as the mean ± standard deviation ($n = 3$). $^{*}P < 0.05$, $^{**}P < 0.01$, compared with the control group.

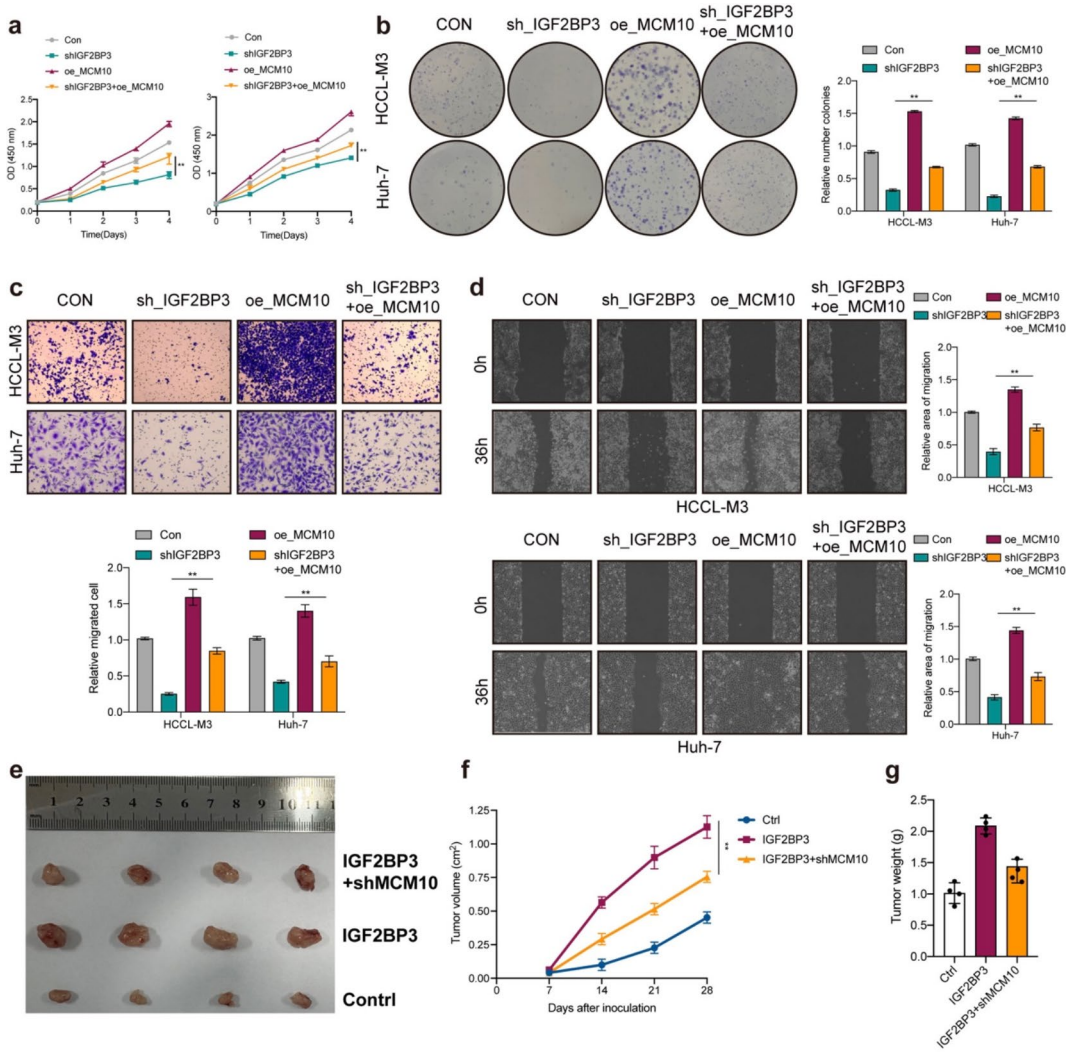

Fig. 7. IGF2BP3 promotes HCC progression through MCM10 expression. (**a**) Cell viability was measured in IGF2BP3 silencing cells with or without overexpression of MCM10 in HCCL-M3 and Huh-7 cells. (**b**) Colony formation assay indicated the rescue effect of MCM10 on IGF2BP3 silencing in HCCL-M3 and Huh-7 cells. (**c**-**d**) Transwell migration assays and wound healing assays were performed in IGF2BP3-deficient cells with or without overexpression of MCM10 in HCCL-M3 and Huh-7 cells. (**e**) The image of mice bearing subcutaneous tumors derived from Huh-7 cells treated with different treatment (Ctrl, IGF2BP3 overexpression, or IGF2BP3 overexpression + MCM10 knockdown) at the indicated times. (**f**) The xenograft growth curves for the IGF2BP3 overexpression, IGF2BP3 overexpression + MCM10 knockdown, and Ctrl groups were plotted by measuring the tumor size (width2 × length × π/6) with a Vernier caliper every 7 days. (**g**) Nude mice were sacrificed, and xenografts were harvested and weighed. All the data are presented as the mean ± standard deviation ($n = 3$). $^{**}P < 0.01$, compared with the control group.

Data availability

Clinical information and high-throughput sequencing-counts were retrieved from the TCGA data portal, which is a publicly available database. The datasets during and/or analyzed during the current study are available from the corresponding author on a reasonable request.

Received: 23 June 2024; Accepted: 4 March 2025
Published online: 10 March 2025

References

1. Zhou, S. L. et al. A positive feedback loop between Cancer Stem-Like cells and Tumor-Associated neutrophils controls hepatocellular carcinoma progression. *Hepatology* **70** (4), 1214–1230 (2019).
2. Li, Q. et al. HIF-1alpha-induced expression of m6A reader YTHDF1 drives hypoxia-induced autophagy and malignancy of hepatocellular carcinoma by promoting ATG2A and ATG14 translation. *Signal. Transduct. Target. Ther.* **6** (1), 76 (2021).
3. Tang, W. et al. The mechanisms of Sorafenib resistance in hepatocellular carcinoma: theoretical basis and therapeutic aspects. *Signal. Transduct. Target. Ther.* **5** (1), 87 (2020).

4. Zaccara, S., Ries, R. J. & Jaffrey, S. R. Reading, writing and erasing mRNA methylation. *Nat. Rev. Mol. Cell. Biol.* **20** (10), 608–624 (2019).
5. Deng, L. J. et al. m6A modification: recent advances, anticancer targeted drug discovery and beyond. *Mol. Cancer*. **21** (1), 52 (2022).
6. Wang, Y. et al. Epigenetic modification of m(6)A regulator proteins in cancer. *Mol. Cancer*. **22** (1), 102 (2023).
7. Huang, H., Weng, H. & Chen, J. m(6)A modification in coding and Non-coding RNAs: Roles and therapeutic implications in Cancer. *Cancer Cell.* **37** (3), 270–288 (2020).
8. Perez-Arnaiz, P., Bruck, I. & Kaplan, D. L. Mcm10 coordinates the timely assembly and activation of the replication fork helicase. *Nucleic Acids Res.* **44** (1), 315–329 (2016).
9. Langston, L. D. et al. Mcm10 promotes rapid isomerization of CMG-DNA for replisome bypass of lagging strand DNA blocks. *Elife* **6**, e29118 (2017).
10. Mayle, R. et al. Mcm10 has potent strand-annealing activity and limits translocase-mediated fork regression. *Proc. Natl. Acad. Sci. U S A*. **116** (3), 798–803 (2019).
11. Alver, R. C. et al. The N-terminus of Mcm10 is important for interaction with the 9-1-1 clamp and in resistance to DNA damage. *Nucleic Acids Res.* **42** (13), 8389–8404 (2014).
12. Chadha, G. S., Gambus, A., Gillespie, P. J. & Blow, J. J. Xenopus Mcm10 is a CDK-substrate required for replication fork stability. *Cell. Cycle*. **15** (16), 2183–2195 (2016).
13. Chattopadhyay, S. & Bielinsky, A. K. Human Mcm10 regulates the catalytic subunit of DNA polymerase-alpha and prevents DNA damage during replication. *Mol. Biol. Cell.* **18** (10), 4085–4095 (2007).
14. Park, J. H., Bang, S. W., Jeon, Y., Kang, S. & Hwang, D. S. Knockdown of human MCM10 exhibits delayed and incomplete chromosome replication. *Biochem. Biophys. Res. Commun.* **365** (3), 575–582 (2008).
15. Wawrousek, K. E. et al. Xenopus DNA2 is a helicase/nuclease that is found in complexes with replication proteins And-1/Ctf4 and Mcm10 and DSB response proteins Nbs1 and ATM. *Cell. Cycle*. **9** (6), 1156–1166 (2010).
16. Yu, W. et al. Identification of Immune-Related LncRNA prognostic signature and molecular subtypes for glioblastoma. *Front. Immunol.* **12**, 706936 (2021).
17. Yang, X. et al. m(6) A-Dependent modulation via IGF2BP3/MCM5/Notch Axis promotes partial EMT and LUAD metastasis. *Adv. Sci. (Weinh)*. **10** (20), e2206744 (2023).
18. Zhou, Y., Zeng, P., Li, Y. H., Zhang, Z. & Cui, Q. SRAMP: Prediction of mammalian N6-methyladenosine (m6A) sites based on sequence-derived features. *Nucleic Acids Res.* **44** (10), e91 (2016).
19. Su, T. et al. Super enhancer-regulated LncRNA LINC01089 induces alternative splicing of DIAPH3 to drive hepatocellular carcinoma metastasis. *Cancer Res.* **83** (24), 4080–4094 (2023).
20. Xia, A. et al. The cancer-testis LncRNA lnc-CTHCC promotes hepatocellular carcinogenesis by binding HnRNP K and activating YAP1 transcription. *Nat. Cancer*. **3** (2), 203–218 (2022).
21. Wan, W. et al. METTL3/IGF2BP3 axis inhibits tumor immune surveillance by upregulating N(6)-methyladenosine modification of PD-L1 mRNA in breast cancer. *Mol. Cancer*. **21** (1), 60 (2022).
22. Hu, Y. et al. Demethylase ALKBH5 suppresses invasion of gastric cancer via PKMYT1 m6A modification. *Mol. Cancer*. **21** (1), 34 (2022).
23. Pan, Z. et al. EWSR1-induced circNEIL3 promotes glioma progression and exosome-mediated macrophage immunosuppressive polarization via stabilizing IGF2BP3. *Mol. Cancer*. **21** (1), 16 (2022).
24. Zhang, N. et al. The m6A reader IGF2BP3 promotes acute myeloid leukemia progression by enhancing RCC2 stability. *Exp. Mol. Med.* **54** (2), 194–205 (2022).
25. Zhang, X. et al. STRIP2 motivates non-small cell lung cancer progression by modulating the TMBIM6 stability through IGF2BP3 dependent. *J. Exp. Clin. Cancer Res.* **42** (1), 19 (2023).
26. Baxley, R. M. et al. Bi-allelic MCM10 variants associated with immune dysfunction and cardiomyopathy cause telomere shortening. *Nat. Commun.* **12** (1), 1626 (2021).

Acknowledgements

The reviewers are grateful for their helpful comments on this article.

Author contributions

All authors contributed to the analysis of data in this study. Conception and design: LZ; Acquisition, analysis, and interpretation of data: LZ, HH, and LL; Writing, review, and/or revision of the manuscript: LZ; Performing the laboratory experiments: LZ, HZ and WF; Administrative, technical, or material support: ZW; Study supervision: ZW. All authors contributed to the article and approved the submitted version.

Funding

This work was supported by the National Natural Science Foundation of China (NO.81960440).

Declarations

Competing interests

The authors declare no competing interests.

Ethics approval and consent to participate

Not applicable.

Consent for publication

Not applicable.

Additional information

Supplementary Information The online version contains supplementary material available at https://doi.org/10.1038/s41598-025-93062-w.

Correspondence and requests for materials should be addressed to Z.W.